THE ASTROPHYSICAL JOURNAL, 417:114–126, 1993 November 1

DISCOVERY OF A THIRD GIANT LOW SURFACE BRIGHTNESS DISK GALAXY[1,2]

D. SPRAYBERRY AND C. D. IMPEY
Steward Observatory, University of Arizona, Tucson, AZ 85721
M. J. IRWIN
Royal Greenwich Observatory, Madingley Road, Cambridge CB3 0EZ, UK
R. G. MCMAHON
Institute of Astronomy, Madingley Road, Cambridge CB3 0HA, UK
AND
G. D. BOTHUN
Department of Physics, University of Oregon, Eugene, OR 97403
Received 1993 February 19; accepted 1993 May 3

ABSTRACT

We report the discovery of a third very large, gas-rich low surface brightness (LSB) disk galaxy, which we designate 1226+0105. Its equatorial coordinates are $\alpha = 12^h26^m39^s.2$ and $\delta = 1°05'38''$ (1950), and it is at a redshift of 23,660 km s^{-1} It exhibits a number of similarities to the previous described examples of this class, Malin 1 (Bothun et al. 1987; Impey & Bothun 1989) and F568-6 (Bothun et al. 1990), in that it has a large total H I mass of $\sim 2 \times 10^{10}\ M_\odot$, a long disk scale length of ~ 14 kpc, a high total luminosity of $M_B = -21.6$, and it harbors an active nucleus. It also shows some striking differences from the previous two. In particular, the newest member of the class shows evidence of pronounced color variations in the disk that are not present in Malin 1 or F568-6. The discovery of this galaxy shows that surveys for LSB galaxies can succeed in finding these giant LSB disks, and the common properties of the three galaxies indicate that they may form a unique class among spirals.

Subject headings: galaxies: individual (1226+0105) — galaxies: peculiar

1. INTRODUCTION

Over the last five years, the study of low surface brightness (LSB) galaxies has revealed a number of surprises. Because LSB galaxies are intrinsically difficult to find, early studies focused on LSB dwarfs in rich cluster environments, such as Virgo (Sandage & Binggeli 1984; Impey, Bothun, & Malin 1988) and Fornax (Davies et al. 1988; Irwin et al. 1990; Bothun, Impey, & Malin 1991). These studies found that the relationship between surface brightness and luminosity becomes weaker at low surface brightness levels, and that the LSB galaxies are significantly bluer than their high surface brightness (HSB) counterparts. Moreover, the Virgo study of Impey et al. was notable for the serendipitous discovery of a LSB background galaxy at 24,750 km s^{-1}. This very low density galaxy, the largest spiral known, was christened Malin 1 (Bothun et al. 1987; Impey & Bothun 1989). Malin 1 has a relatively normal bulge and an unusually large LSB disk. Since then, one other similar galaxy, known as F568-6, has been reported by Bothun et al. (1990). This galaxy was found during a search of LSB objects on the Second Epoch Palomar Sky Survey plates by Schombert et al. (1992; Schombert & Bothun 1988). Their search uncovered a number of interesting LSB galaxies, and they designated 20 galaxies having radial velocities $\gtrsim$10,000 km s^{-1} as possible "Malin cousins," although photometric and spectroscopic data have not yet been collected for most of these objects.

Surface photometry shows that both Malin 1 and F568-6 have extremely large disk scale lengths and therefore large total luminosities, despite their low disk surface brightnesses. Both also have large total H I masses. Finally, both galaxies have large but isolated H II regions, indicating that there are some areas of active star formation embedded in disks that are otherwise smooth and quiescent. The smoothness of the underlying disk and the apparently slow rate of overall star formation stimulated a theoretical description by Hoffman, Silk, & Wyse (1992) of how such disks could form from isolated 3 σ fluctuations in the density background. Their model predicts that such galaxies should have normal spiral bulges, with large, low-density, gas-rich disks which show little evidence of evolution.

In this paper we report the discovery of a third giant LSB disk galaxy, 1226+0105, and present a preliminary description of the properties of this galaxy. The total H I mass and total B luminosity of 1226+0105 are virtually identical to those of F568-6, and within a factor of 2 of those of Malin 1. We find 1226+0105 also has several H II regions in its outer disk, indicating active but localized star formation at the current epoch. The bulge metallicity of 1226+0105 is very similar to that of both Malin 1 and F568-6, and like both of them it also shows evidence of an active galactic nucleus. Unlike them, however, 1226+0105 has an active nucleus with both broad and narrow line components, suggesting a more complex nuclear structure. It is also distinguished by photometric evidence of localized red and blue stellar populations in its disk,

[1] The optical observations reported here were obtained with the Multiple Mirror Telescope, a facility jointly operated by the Smithsonian Institution and the University of Arizona, and the William Herschel Telescope operated on the island of La Palma by the Royal Greenwich Observatory in the Spanish Observatorio del Roque de los Muchachos of the Instituto de Astrophysica de Canarias.

[2] Radio observations were obtained with the 305 m telescope at Arecibo. The Arecibo Observatory is part of the National Astronomy and Ionsphere Center, which is operated by Cornell University under a cooperative agreement with the National Science Foundation.

suggesting a more varied star formation history. These differences expand the galaxy parameter space occupied by giant LSB disks and so illuminate further the extent of our ignorance of the true range of galaxy properties.

In the next section we briefly describe how 1226+0105 was found. Section 3 details the surface photometry results and compares them to Malin 1 and F568-6. Section 4 presents the optical and radio spectroscopy of the new galaxy in comparison to its two predecessors. Section 5 contains the discussion of the findings and their implications for the star formation history of 1226+0105, and the impact on the current theory of LSB disk formation.

2. DISCOVERY

1226+0105 was discovered as part of a new equatorial survey of LSB galaxies around the $\delta = 0°$ strip. Full details of this survey will be reported elsewhere, but a brief description will illustrate the problems involved in finding such objects.

Target LSB galaxies were identified by using a combination of both automated and eyeball searches of glass copies of UK Schmidt telescope (UKST) IIIaJ survey plates. To date, more than 30 equatorial fields, covering $\sim$1000 square degrees of sky, have been surveyed and the candidate LSB galaxies weeded out from a total of well over 10^7 images in the strip.

The Automated Plate Measuring (APM) facility at Cambridge[3] was used to locate all objects on a plate meeting two criteria: first, they must have a size of 0.2 mm $\leq D_{25} \leq$ 3.0 mm (or about 13″ $\leq D_{25} \leq$ 200″), where D_{25} is the diameter at an effective surface brightness of 25 mag arcsec^{-2}; and second, they must have an average surface brightness of $\mu_B \gtrsim 23$. The objects revealed by the scan are then reviewed by eye to eliminate as many previously cataloged galaxies, plate flaws, Galactic cirrus clouds, and other interlopers as possible. A description of the APM facility can be found in Kibblewhite et al. (1984).

The eyeball search was carried out independently of the automatic scan using a combination of low-power ($\times$5) binocular microscope and direct eye search. Each plate was searched in lanes $\sim$5 cm wide and any LSB feature or galaxy with unusual extended morphology noted. Straightforward use of a 40 cm graduated rule sufficed to locate the candidates to within 0.5 mm with respect to the plate edges. Then simple application of the known plate center, scale, and orientation enabled these "x-y" coordinates to be translated into celestial coordinates with an accuracy of better than 1′. These celestial coordinates were sufficiently accurate that the images could then be routinely measured (in the form of two-dimensional pixel maps) using the APM and at the same time accurate ($\sim$1″) coordinates found. It is worth pointing out that in doing an eyeball search for LSB galaxies, use of glass copies greatly facilities matter because (1) the background density is adjusted during copying to be roughly 0.5 D, typically half the original plate background density; (2) a modest amount of contrast enhancement around sky background is also folded in, which in conjunction with (1) makes LSB features easier to see; and (3) the plates are readily available.

Objects selected by eye are then combined with the machine-selected sample in a master list of candidates for followup CCD photometry, optical spectroscopy, and 21 cm radio observation. The eyeball search is a necessary adjunct to the automated scanning because the global parametric requirements of the automatic search cannot be guaranteed to pick out all galaxies of manifestly unusual morphology. An excellent illustration of this problem is provided by 1226+0105. The prominent nuclear component of the galaxy outweighs the contribution of the LSB disk detected at the analysis isophote (25 mag arcsec^{-1}), causing the apparent "mean" surface brightness to fall on the wrong side of the surface brightness selection boundary. Although given the benefit of hindsight it is possible to try to generalize the automatic selection criteria to cope with cases like this, and presumably others, eventually it becomes self-defeating. The selection criteria become too complicated to readily interpret in terms of easily measurable galactic properties, and there is never a guarantee of picking all interesting types. It is more logical to use the eyeball search as the primary candidate selection and use the machine-selected sample to guarantee that one is complete to some simple well-defined selection boundaries.

As noted before 1226+0105 was picked out by eye as a likely Malin 1–type candidate. It lies in UKST field 860 at $\alpha = 12^h26^m39^s.2$ and $\delta = 1°05'38''$ (1950), in a region of sky occupied by the southern extension of the Virgo cluster. Its apparent diameter at the detection limit of the APM scan ($\sim$25 mag arcsec^{-2}) is 0.′56 (0.5 mm at the UKST plate scale of 67.″12 mm^{-1}). A gray-scale reproduction of the V-band CCD image is shown in Figure 1. The gray-scale limits in Figure 1 were set to provide the best contrast in the spiral arms and to enhance the LSB features in the disk; the scale limits cause the slightly elongated bulge to appear completely saturated. Apart from the fairly bright but marginally resolved nucleus and the inner portions of the spiral arms, the outer disk of the galaxy, which extends to a radius of $\gtrsim$45″ (§ 3), is almost invisible against the sky background.

It was clearly the combination of the LSB disk and the small, bright bulge component that led to 1226+0105 being selected by eye. It is outside the scope of this paper to discuss issues regarding completeness of surveys for this type of object (including both Malin 1 and F568-30), but it is worth noting that even surveys specifically aimed at finding LSB disks will almost certainly miss a large proportion of such objects (see Bothun et al. 1987), in part due to the strong selection bias in favor of face-on LSB disk showing some evidence of recent, albeit modest, star formation.

3. SURFACE PHOTOMETRY

CCD images of 1226+0105 were obtained at the Steward Observatory 2.3 m telescope on 1992 May 2, using the Loral 2048 × 2048 CCD in direct imaging mode and Johnson B and V and Kron-Cousins R colored glass filters. The CCD was binned 2 × 2 on-chip, giving a pixel scale of 0.″3 pixel^{-1} and a field of view 5′ on a side. Standard IRAF tasks were used for data reduction and photometric calibration, and standard stars from the lists of Christian et al. (1985), which also use the Johnson B and V and Kron-Cousins R system, were used for the photometric reference points.

The one-dimensional radial intensity profile of 1226+0105 (in intensity per pixel) was measured by fitting elliptical isophotes to the reduced and sky-subtracted images using the algorithm described by Jedrzejewski (1987). This algorithm yields the average intensity around each elliptical isophote, allowing a one-dimensional radial profile to be plotted simply as average intensity versus semimajor axis. Standard trans-

[3] The APM is a National Astronomy Facility, at the Institute of Astronomy, operated by the Royal Greenwich Observatory.

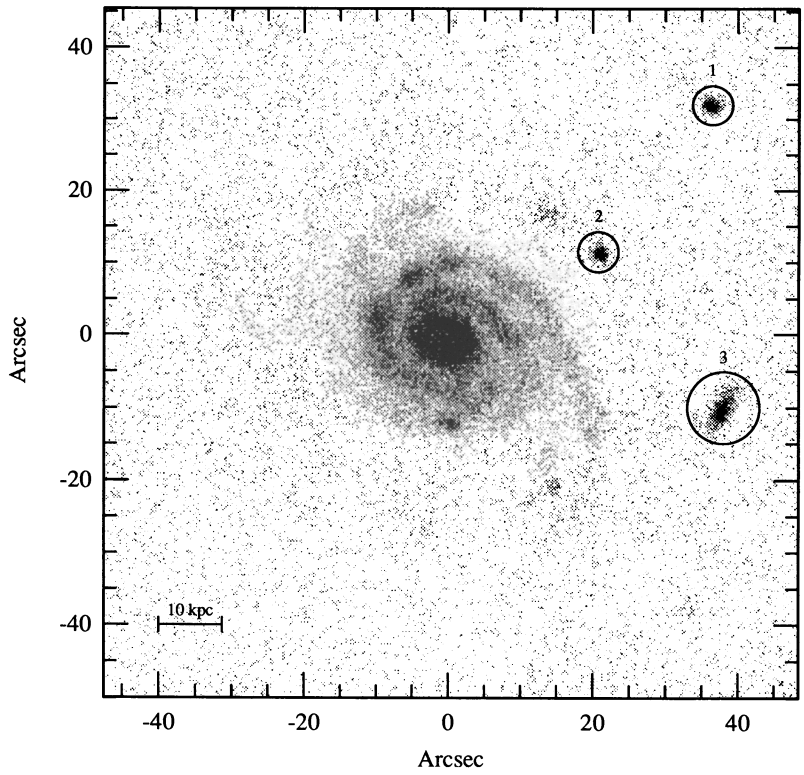

FIG. 1.—Central portion of V-band CCD image of 1226+0105. North is up and East is to the left. The scale is 0".3 pixel^{-1}. Gray-scale limits were set to provide maximum contrast in the spiral arms, causing the slightly elongated bulge to appear saturated. The bright regions enclosed in circles are the probable giant star-forming regions referred to in the text. The area depicted here is ~1.34 mm square on the UK Schmidt plate. The scale bar shows the physical scale of the photograph, assuming $H_0 = 100$ km s^{-1} Mpc^{-1}.

formation equations (Hardie 1962) were used to calibrate the intensity profiles to surface brightness in mag arcsec^{-2}. The radial surface brightness profile are shown in Figure 2*a*. The transformation equations also provide colors at each isophote, and the resulting color profiles appear in Figure 2*b*. The surface brightness and surface colors in Figure 2 are corrected by a factor of $(1 + z)^4$ to account for the effects of cosmic expansion on surface brightness. The method outlined by Burstein & Heiles (1978) was used to correct for local Galactic reddening. K-corrections of Sbc galaxies from the tabulations of Coleman, Wu, & Weedman (1980) were also applied. Use of the K-corrections of Scd galaxies from the same tabulations would yield identical colors at this redshift, while the K-corrections of E/S0 galaxies would yield colors that are bluer by 0.15 mag in $B-V$ and 0.05 mag in $V-R$. Because these K-corrections are applied uniformly to the entire galaxy, use of a different morphological type for determining the K-correction would not affect the discussion below of color variations within the disk of 1226+0105.

Accurate estimation of the sky value is critical when trying to measure surface brightnesses that are themselves a tiny fraction of the sky brightness. We estimated the sky intensity in these images by finding the modes of the pixel intensity distributions in the four corners, discarding the highest and lowest of these four values, and then adopting the average of the remaining two values as the sky intensity. The profiles in Figure 2 are marked to show the effects of both statistical uncertainties and systematic errors in the sky estimate. The inner errors bars indicate the internal uncertainties, which include the statistical uncertainty in our best estimate of the sky intensity. The outer tick marks indicate the systematic effect on the profile of changing the sky level estimate by the maximum likely error, as determined by the difference between the adopted sky intensity and the most extreme outlier among the four corner values.

The one-dimensional radial surface brightness profiles resulting from the isophote fitting routine were decomposed into bulge and disk components in a three-step process. First, a least-squares routine was used to fit a radial exponential luminosity profile, over the range from 14" to 42" in semimajor axis. The exponential model was then subtracted from the measured intensity distribution and a least-squares fit to a de Vaucouleurs profile (surface brightness versus $r^{1/4}$) over the range from 1" to 6" in semimajor axis was made. The profile point at 0" in Figure 2*a* represents the surface brightness of the central pixel. The seeing disk of ~1".25 spreads out the central intensity peak of the bulge and causes this "isophote" to be systematically too faint. For this reason, it was not used in fitting the de Vaucouleurs model. This procedure was applied to the images in all three filters. The results of the fits are shown in Figure 2*a* and reported in Table 1, along with comparable information, where available, for Malin 1 and F568-6. In Table 1, and throughout this paper, all distance dependent calculations use $H_0 = 100$ km s^{-1} Mpc^{-1}. The disk parameters are projected central surface brightness and exponential scale length. The bulge parameters are the "effective radius," defined as the semimajor axis enclosing half the total bulge luminosity, and the surface brightness at the effective radius. The disk and bulge absolute magnitudes were obtained by integrating the fitted models to infinity. The disk fitting region of 14"–42" in

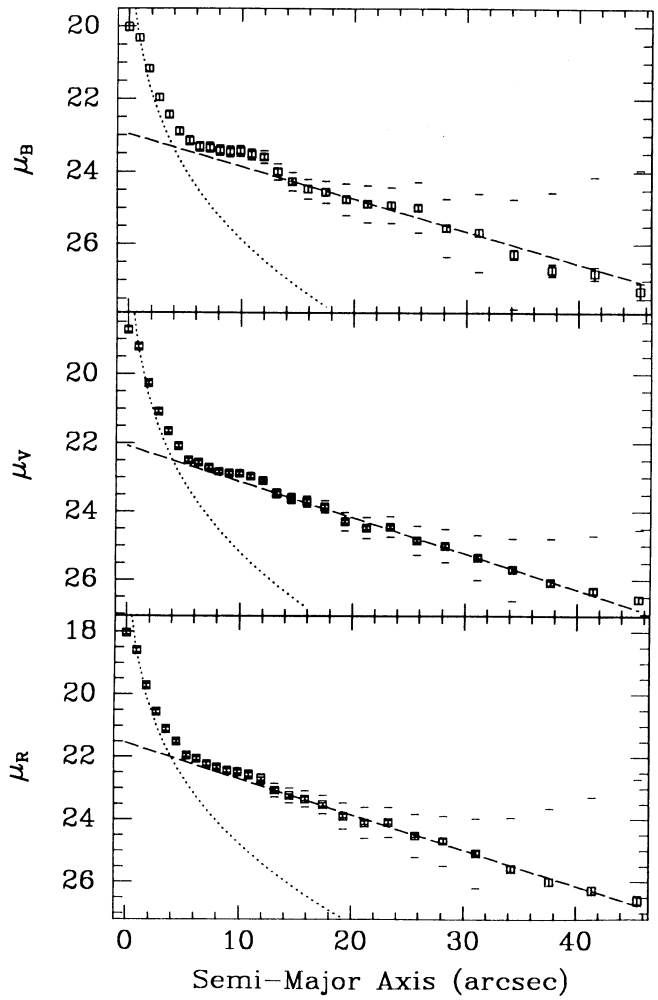

FIG. 2a

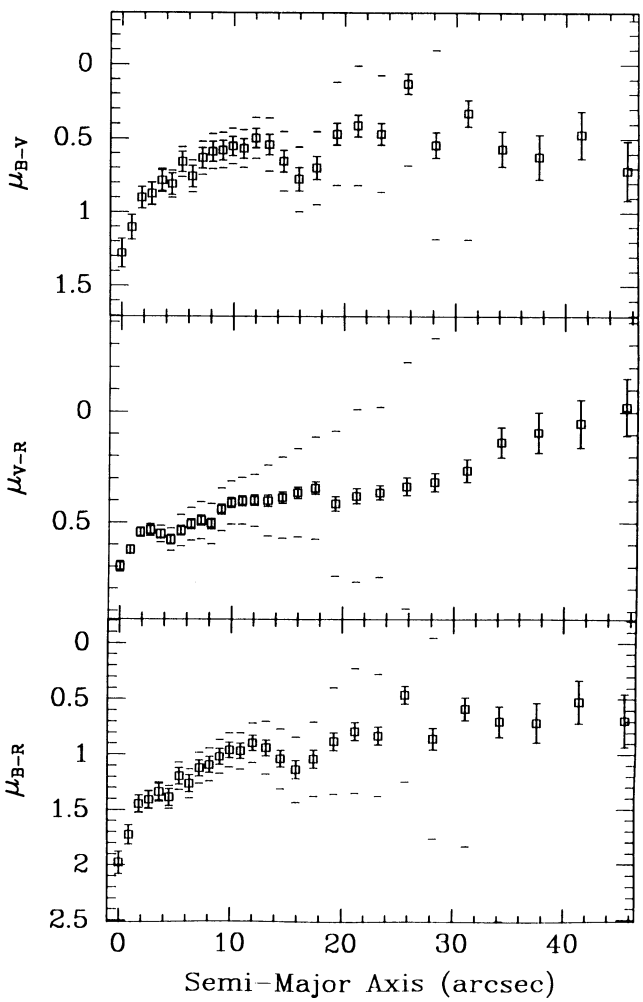

FIG. 2b

FIG. 2.—(*a*) Radial surface brightness profiles of 1226+0105. *B* is at the top, *V* is in the middle, and *R* is at the bottom. The dashed line shows the best-fit exponential disk model, and the dotted line shows the best-fit de Vaucouleurs bulge model. The inner error bars (which in most cases are smaller than the size of the plotted points) show the internal uncertainties in the isophotal surface brightnesses. The outer tick marks at each semimajor axis show the systematic effect of over- or undersubtraction of sky flux. (*b*) Radial surface color profiles of 1226+0105. $B-V$ is at the top, $V-R$ is in the middle, and $B-R$ is at the bottom. $B-R$ is simply the sum of the other two profiles. As with Fig. 5*a*, the inner error bars show the internal uncertainties for each point, and the outer tick marks show the systematic effect of over- or undersubtraction of sky flux.

semimajor axis was chosen to avoid the pronounced flattening of the *B* and *V* profiles between 7″ and 14″. The flattened region represents the inability of the isophote fitting routine to follow the rapid changes in intensity between the bright, inner portions of the spiral arms and the much fainter interarm regions (see Fig. 1). Figure 3 shows the isophotal ellipticities (Fig. 3*a*) and position angle (Fig. 3*b*) as functions of semimajor axis. Both parameters change abruptly and have large uncertainties over the range of 7″–14″, indicating that elliptical isophotes are a poor model for the brightness distribution there. Fits were also performed using the entire region from 7″ to 42″ semimajor axis for comparison, but the results were still within the upper and lower limits obtained by fitting only the region for 14″ to 42″.

Three large, bright regions are enclosed within circles in Figure 1. Aperture photometry (using aperture sizes roughly equal to the sizes of the circles drawn in Fig. 1) of these regions shows that their total luminosities are quite large; the absolute *V*-magnitudes are $M_V = -16.34$, $M_V = -16.37$, and $M_V = -17.30$ for regions 1, 2, and 3, respectively, assuming that they lie at the same distance as 1226+0105. The apparent magnitudes and colors for these regions are summarized in Table 1. Absent spectroscopic confirmation of their redshifts, these regions can only tentatively be considered as part of 1226+0105. Indeed, it is likely that Region 1 is not associated with this galaxy, as it is redder than the other two and has a red core (see Fig. 4*a*) suggestive of the galactic bulge, and it lies outside the outermost isophote. Also, Region 3 is somewhat elongated, and the elongation is almost perpendicular to the local direction of the nearest spiral arm, suggesting that it may be an inclined spiral galaxy behind 1226+0105. If these regins are part of 1226+0105, then each region has broad-band luminosities comparable to those of Local Group irregular galaxies such as NGC 205 and the Small Magellanic Cloud, yet they are embedded within a huge, LSB, gas-rich galactic disk. Despite their large luminosities, however, Regions 1 and 2 contribute $\lesssim 1\%$ of the total luminosity of 1226+0105, and Region 3 contributes $\sim 2\%$ of the total. Bothun et al. (1990) noted that a

TABLE 1

PHOTOMETRIC PROPERTIES

Component	Filter	Parameter	Malin 1	F568-6	1226+0105
Disk	B	α	55.0	16.0	14.0 ± 1
		μ_0	26.5	23.5	23.2 ± 0.2
		M	-20.8	-21.1	-21.0 ± 0.3
	V	α	~ 55.0	...	11.9 ± 0.6
		μ_0	25.7 ± 0.1	...	22.1 ± 0.1
		M	...	...	-21.5 ± 0.2
	R	α	...	...	10.9 ± 0.4
		μ_0	...	...	21.6 ± 0.1
		M	...	...	-21.9 ± 0.1
		$(B-V)$	0.8 ± 0.1	0.55 ± 0.05	0.5 ± 0.3
		$(V-R)$	...	...	0.3 ± 0.2
Bulge	B	$r_{\rm eff}$	3.9	1.8	2.5 ± 0.1
		$\mu_{\rm eff}$	...	...	22.2 ± 0.2
		M	-19.7	-19.7	-20.0 ± 0.2
	V	$r_{\rm eff}$	~ 4.0	...	1.8 ± 0.1
		$\mu_{\rm eff}$	22.2 ± 0.2	...	20.4 ± 0.1
		M	...	...	-20.9 ± 0.1
	R	$r_{\rm eff}$	...	...	1.6 ± 0.1
		$\mu_{\rm eff}$	...	...	19.6 ± 0.1
		M	...	...	-21.5 ± 0.1
		$(B-V)$	0.95 ± 0.02	...	0.9 ± 0.3
		$(V-R)$	...	...	0.6 ± 0.2
Region 1	V	m	...	...	20.53 ± 0.06
		$(B-V)$	...	...	0.9 ± 0.1
		$(V-R)$	...	...	0.58 ± 0.04
Region 2	V	m	...	...	20.50 ± 0.05
		$(B-V)$	...	...	0.39 ± 0.08
		$(V-R)$	...	...	0.26 ± 0.04
Region 3	V	m	...	...	19.57 ± 0.05
		$(B-V)$	...	...	0.48 ± 0.08
		$(V-R)$	...	...	0.42 ± 0.03

NOTES.—α and $r_{\rm eff}$ are in kpc. μ_0 and $\mu_{\rm eff}$ are in mag arcsec^{-2}. M, $(B-V)$, and $(V-R)$ are in magnitudes.

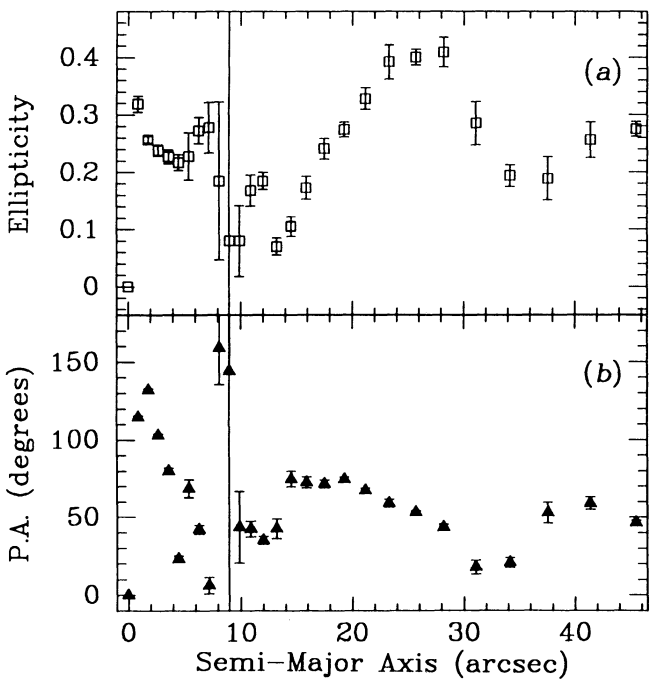

FIG. 3.—Ellipticity (*a*) and position angle (*b*) as a function of semimajor axis. The region between 7″ and 15″ where the parameters are poorly determined corresponds to the flattened portion of the B and V profiles in Fig. 2*a*.

similarly striking complex of H II regions existed within the disk of F568-6. Such large but isolated region of apparent star formation thus seem to be a characteristic of this class of giant LSB disk galaxies.

The inclination of the disk was estimated by refitting the isophotes after manually setting the pixel values to zero at the locations of the apparent H II regions, which are enclosed within circles in Figure 1. The isophote fitting routine ignores pixels with a value of exactly zero, so these isophotes exclusively reflect the smooth component of the disk. The average of the ellipticities of the "smooth component" isophotes from 20″ to 45″ semimajor axis is 0.27 ± 0.08. Assuming that this ellipticity is due entirely to inclination of a circular disk leads to the estimated inclination of $43° \pm 6°$. However, the optical disk of this galaxy is manifestly not a uniform circle, and the elliptical isophotes trace the actual spiral arm structure imperfectly. Thus, the true uncertainty in the inclination must be larger than the scatter in the isophotal ellipticities.

Despite the similarity in the global properties of 1226+0105, F568-6, and Malin 1, there is a striking difference between 1226+0105 and F568-6 in their color profiles. The color profiles for 1226+0105 (Fig. 2*b*) show the following: an extremely red nucleus, $B-V > 1.5$; a bulge of relatively normal color, $B-V \sim 1$, albeit with some contamination from the nuclear reddening (see § 4.1 for a detailed discussion of the nuclear reddening) and small seeing differences between frames; and a blue disk with $B-V \sim 0.5$. There are also significant fluctua-

1993ApJ...417..114S

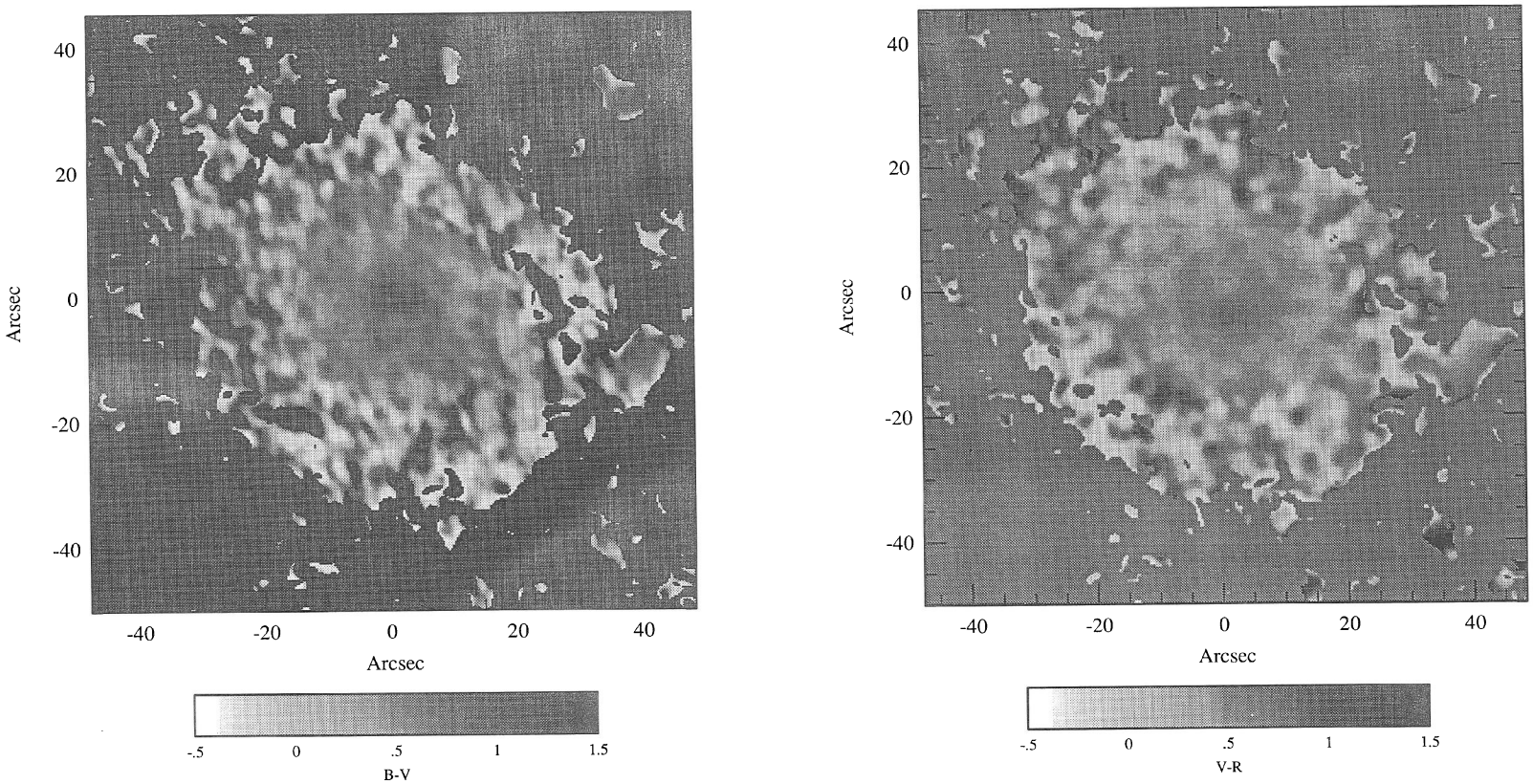

FIG. 4.—(*a*) $B-V$ color map of 1226+0105. All pixels with errors greater than 0.9 mag have been set to the $B-V$ color of the sky; these pixels, and the pixels that have flux levels indistinguishable from that of the sky, make up the uniform gray background, The pixel scale and orientation are identical to Fig. 1. Note the interspersing of red and blue areas in the outer disk, and the tracing of spiral arms by the blue regions in the inner and middle disk. (*b*) $V-R$ color map of 1226+0105. All pixels have errors less than 0.06 mag. Pixels with flux levels indistinguishable from that of the sky have been set to the $V-R$ color of the sky; they make up the uniform gray background. Pixel scale and orientation are identical to Fig. 1. Note that the pattern of interspersed region and blue regions is generally similar to that of Fig. 3*a*, though some regions differ in extent between the two maps.

1993ApJ...417..114S

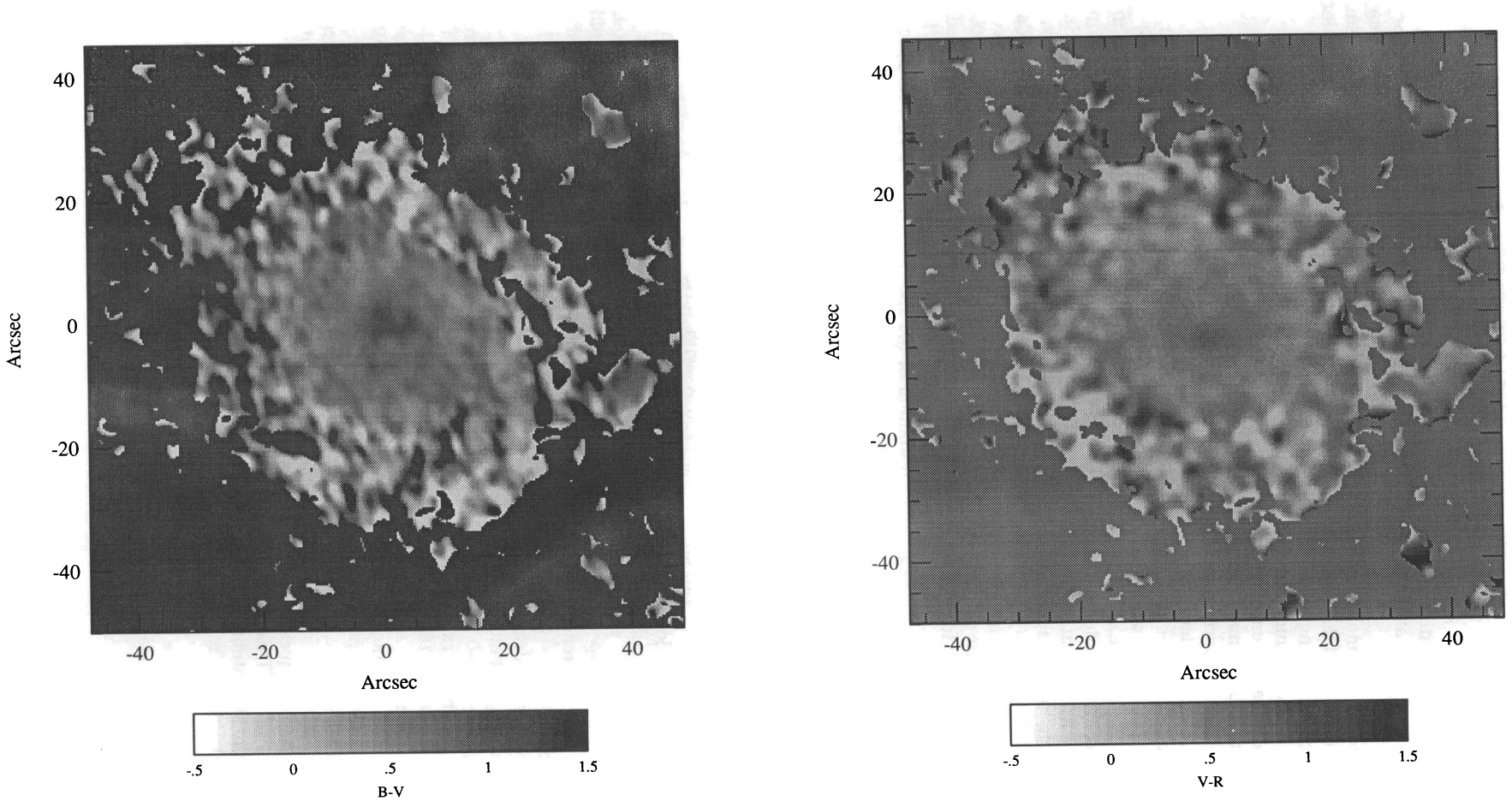

FIG. 4.—(*a*) $B-V$ color map of 1226+0105. All pixels with errors greater than 0.9 mag have been set to the $B-V$ color of the sky; these pixels, and the pixels that have flux levels indistinguishable from that of the sky, make up the uniform gray background, The pixel scale and orientation are identical to Fig. 1. Note the interspersing of red and blue areas in the outer disk, and the tracing of spiral arms by the blue regions in the inner and middle disk. (*b*) $V-R$ color map of 1226+0105. All pixels have errors less than 0.06 mag. Pixels with flux levels indistinguishable from that of the sky have been set to the $V-R$ color of the sky; they make up the uniform gray background. Pixel scale and orientation are identical to Fig. 1. Note that the pattern of interspersed region and blue regions is generally similar to that of Fig. 3*a*, though some regions differ in extent between the two maps.

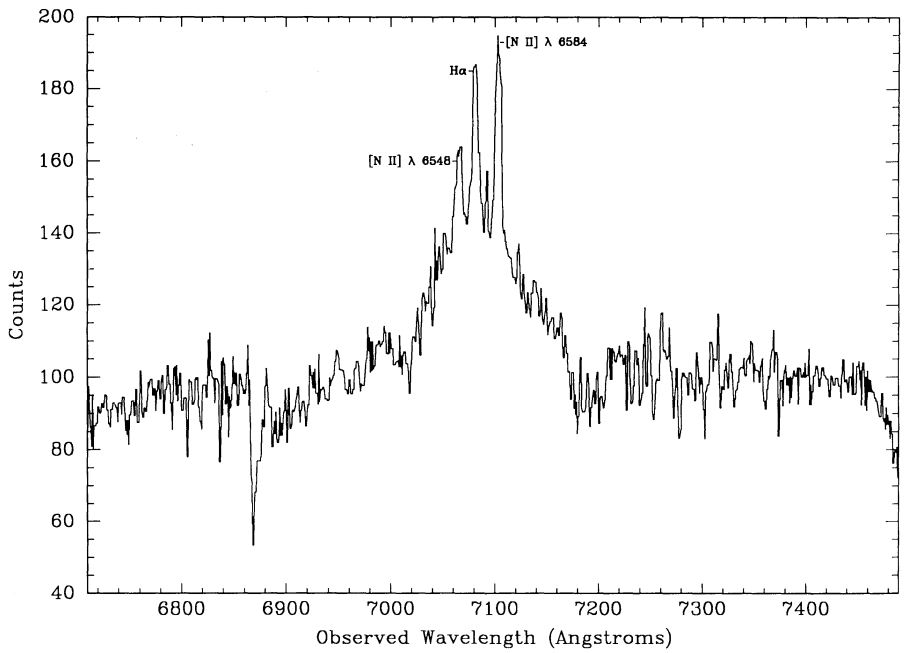

FIG. 5.—High-resolution nuclear spectrum of 1226+0105. Resolution is ~2 Å (0.74 Å pixel^{-1}). The narrow emission lines discussed in the text are identified. The asymmetric broad Hα line is directly below the three narrow lines.

Malin 1 nor F568-6 showed a broad Hα component comparable to the one present in 1226+0105. The Hα FWZI of ~9000 km s^{-1} places 1226+0105 in the lowest 10% of the distribution of widths observed by Osterbrock (1977) for Seyfert I galaxies. In contrast, the FWZI for Malin 1 and F568-6 are both below the cutoff at ~6000 km s^{-1} noted by Osterbrock.

There is convincing evidence of reddening of the active nucleus. First, the continuum visible in Figure 6 is very red with $F_\nu \propto \nu^{-2}$. Second, despite the strong Hα line mentioned above, there is no clear detection of Hβ. There is what seems to be a weak broad emission line at about 5214 Å, but if it is Hβ, then its redshift differs by about 1800 km s^{-1} from that of all the other emission lines. The intensity ratio Hα/Hβ would be expected to be $\lesssim 3$ if purely recombination conditions exist (Osterbrock 1989), or as high as 5 or 6 if the electron densities are sufficient (~10^8 cm^{-3}) to make collisional excitation and Balmer self-absorption significant (Osterbrock, Koski, & Phillips 1976). Using the rms of the spectrum centered on 5246 Å

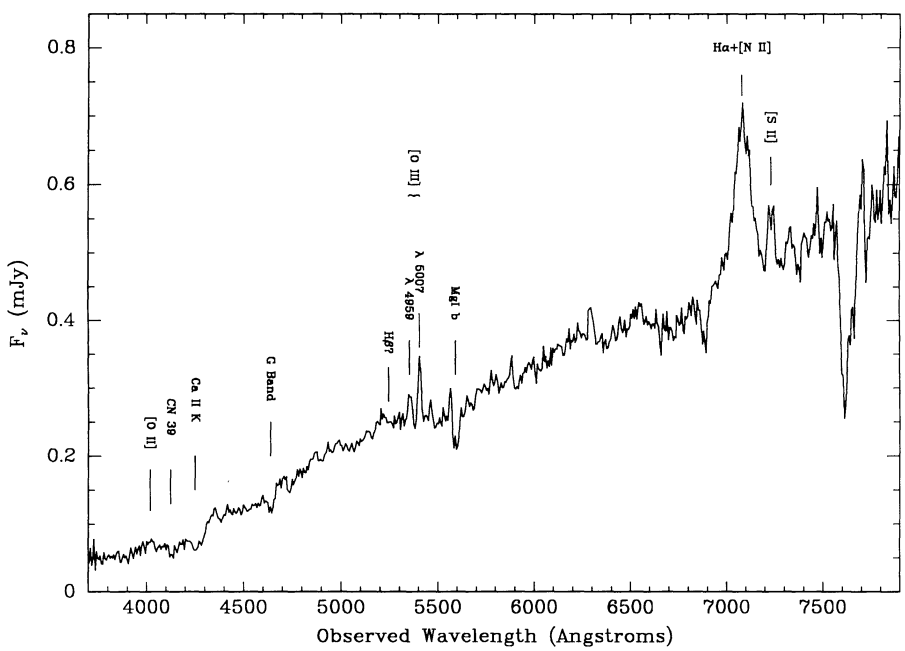

FIG. 6.—Low-resolution nuclear spectrum of 1226+0105. Resolution is ~20 Å (6.3 Å pixel^{-1}). Spectral features discussed in the text are identified. The identifier "Hβ?" indicates where the Hβ emission should be to match the redshift of the Hα emission.

TABLE 2

EMISSION-LINE PROPERTIES

Line EW (Å)	Malin 1	F568-6	1226+0105
[O II] λ3727	21.9	...	7.4[a]
[O III] λ4959	2.2	...	4.8[a]
[O III] λ5007	1.7	...	7.8[a]
Hα + [N II]	15.4	6.4	63.2[a]
[N II] λ6548	...	...	1.33[b]
Hα (narrow)	...	...	2.21[b]
[N II] λ6584	...	...	2.73[b]
Hα (broad)	...	...	59.36[b]
[S II] λλ6717, 6731	7.1	2.2	6.1[a]
FWZI Hα + [N II] (km s^{-1})	5800	5300	8970[c]
Line Flux (ergs cm^{-2} s^{-1})[d]	**Malin 1**	**F568-6**	**1226+0105**
[O II] λ3727	2.5×10^{-16}	...	8.4×10^{-16}
[O III] λ4959	9.5×10^{-17}	...	1.2×10^{-15}
[O III] λ5007	7.0×10^{-17}	...	2.0×10^{-15}
Hα + [N II]	6.0×10^{-16}	...	1.7×10^{-14}
[S II] λλ6717, 6731	3.2×10^{-16}	...	1.7×10^{-15}

a Measured from MMT spectrum, ~20Å resolution.

[b] Measured from WHT spectrum, ~2 Å reslution. Total does not exactly match corresponding unresolved lines from MMT spectrum due to resolution difference.

[c] Measured from WHT spectrum.

[d] All fluxes for 1226+0105 measured from MMT spectrum.

(where Hβ should be) and assuming Hβ would have the same velocity width (FWZI) as Hα (N110 Å), the 2 σ upper limit on Hβ flux is $\sim 1.7 \times 10^{-15}$ ergs cm^{-2} s^{-1} which gives a lower limit on Hα/Hβ of ~10. Reddening therefore reduces the nuclear flux by a factor of 2 or more between 4861 Å (in the rest frame of the galaxy) and 6563 Å. Because the slit covers both the AGN and a substantial fraction of the galactic bulge, it is impossible to say whether the reddening effects only the AGN emission or whether the bulge starlight is also reddened. The reddening of the nuclear spectrum is severe enough that no firm conclusions about the conditions within the AGN line-emitting regions can be drawn from the emission-line ratios.

4.1.2. *Absorption Line Indices*

The Mg_2, CN, and G 4300 indices defined by Burstein et al. (1984) are reported in Table 3, and they indicate that 1226+0105 lies in the range of intermediate metallicity between the Galactic globular clusters studied by Burstein et al. and the elliptical galaxies Burstein et al. used as a baseline. 1226+0105 thus has a somewhat lower bulge metallicity than does Malin 1, which Impey & Bothun (1989) found to lie at the high end of Burstein's metallicity range for ellipticals.

TABLE 3

ABSORPTION LINE INDICES

Line	Malin 1	F568-6	1226+0105
EW Ca II K λ3933 (Å)	9.7	...	4.4
EW G band λ4304 (Å)	8.0	...	4.7
EW Mg I λ5180 (Å)	5.0	4.7	5.8
EW Na I λ5895 (Å)	5.8	6.0	...
Mg_2[a] (mag)	0.29	...	0.18
CN[b] (mag)	...	...	0.03
CN39[c] (mag)	0.54	...	0.28

[a] As defined by Burstein et al. 1984; identical to Mg*b* as defined by Boroson 1980.

[b] As defined by Burstein et al. 1984.

[c] As defined by Boroson 1980.

Boroson (1980) has studied the stellar populations in spiral bulges using two line indices. One, CN39, measures the strength of the broad trough due to CN around 3860 Å; the index is reported in Table 3. The other, which he called Mg*b*, is virtually identical to the Mg_2 index of Burstein et al. The indices for 1226+0105 are plotted in Figure 7, along with Boroson's data for spiral bulges and the corresponding data for Malin 1. 1226+0105, like the other spiral bulges, shows too weak a CN39 index for its metallicity (which the Mg*b* index presumably tracks), in comparison to the average values for elliptical galaxies (plotted as the dashed line in Fig. 7). The relative weakness of CN39 in comparison to Mg*b* indicates the presence of some sort of blue continuum light which dilutes the CN39 index more severely than the Mg*b* index. The presence of this blue continuum is the clearest lesson to be learned from Figure 7; what Figure 7 does not make clear is the source of that blue continuum. Boroson proposed that this continuum came from a population of younger, hotter stars and suggested a method of moving a galaxy upwards along an addition vector (parallel to the solid line in Fig. 7) to determine how much of the continuum at 4500 Å would be due to stars of type earlier than G0. If the method of Boroson is applicable, the fraction of light at 4500 Å due to these younger stars would be ~40%, slightly higher than the ~30% estimated for Malin 1 by Impey & Bothun (1989). However, Boroson's method may not be truly applicable in this case: the relative weakness of the CN39 index could be due to a power-law continuum if one is present. A power law that contributed 40% of the flux at 4500 Å would contribute 67% (for a power-law index of −1) or 60% (for a power-law index of −2) of the flux at 4000 Å, and it would still contribute 29% (index = −1) or 36% (index = −2) of the flux at 5600 Å. Thus, a reasonable power-law component could at least partly account for the relative strengths of the Mg*b* and the CN39 indices, without invoking any separate population of young stars. Impey & Bothun (1989) reached a similar conclusion about Malin 1. The metallicity difference, as indicated by the Mg*b* index, between Malin 1 and 1226+0105

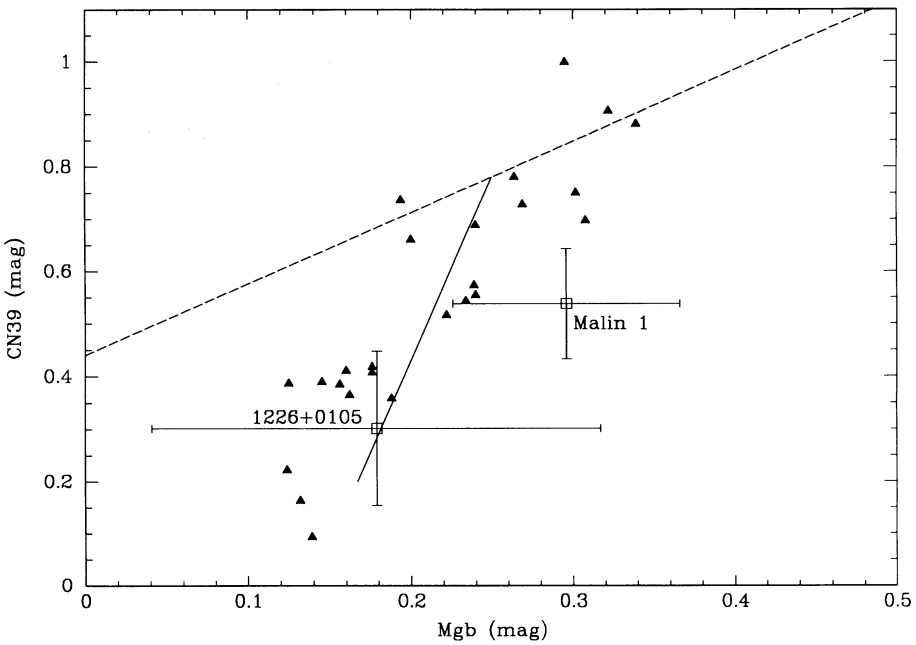

FIG. 7.—CN39 and Mg*b* indices plotted for 24 spiral bulges from Boroson (1980), along with Malin 1 and 1226+0105. The dashed line indicates the mean relationship found by Boroson for elliptical galaxies, and the solid line is the vector for addition of a hot star component.

is $\sim 1\ \sigma$ before correction for any contaminating blue continuum. Of course, if the power-law continuum has a different slope from that of Boroson's proposed population of younger stars, the vector for addition or subtraction of this continuum would have a different slope from that of the solid line in Figure 7. If any power-law continuum had a steeper slope in 1226+0105 than in Malin 1, then the true metallicity difference between the two would be less. As noted by Impey & Bothun (1989), separating the spectral contributions of the active nucleus and the starlight is impossible without some independent estimate of the continuum due to the active nucleus. Furthermore, as noted in § 4.1.1, the active nucleus of 1226+0102 is almost certainly heavily reddened, which further complicates any attempt to separate the spectral contribution of the AGN from that of the stars.

4.2. *Radio*

We obtained a 21 cm spectrum of 1226+0105 at the 305 m Arecibo radio telescope in 1992 May. Three pairs of scans were taken in succession, using the 22 cm circular feed tuned to a central frequency of 1316 MHz to accommodate the redshift previously determined from optical spectroscopy. Each pair was taken by tracking and integrating on the source for 5 minutes, then slewing the telescope beam to the altitude and azimuth where the on-source integration began, and tracking and integrating on this off-source position for 5 minutes to obtain a background sky measurement. Data reduction and calibration were performed on-site using the National Astronomy and Ionosphere Center's standard GALPAC software. This spectrum appears in Figure 8.

The H I spectrum of 1226+0105 shows a double-peaked profile, indicating a rotating spiral disk. As with F568-6, the peaks are not even. As with F568-6 and Malin 1, the corrected line width is high, indicating rapid rotation. The H I mass is also very close to that of F568-6. The H I properties of 1226+0105, Malin 1 and F568-6 are summarized in Table 4. The line widths are the rest widths at 20% of the mean flux value, corrected for inclination. The 1 σ error reported on the corrected line width for 1226+0105 is largely due to the uncertainty in the inclination. The H I mass for 1226+0105 is a lower limit, due to the possibility of partial resolution of the galaxy by the 3.3 Arecibo beam. Using the $\mu_B = 27$ mag arcsec^{-2} isophote to define the optical edge of the galaxy, the optical diameter is 1.3. In many spirals, including Malin 1 (van Gorkom, Bothun, & Impey 1993) and F568-6 (Bothun et al. 1990), the H I extends far beyond the optical diameter, and if the gas in 1226+0105 extends further than ~ 2.5 times the optical radius (which appears to be the case for Malin 1 and F568-6), then the Arecibo beam would miss some of the H I signal. Table 4 also includes an estimate of the total dynamical mass of 1226+0105. This rough estimate assumes a Brandt rotation law with a flat index ($n = 1.3$), in the manner described by Haynes & Giovanelli (1984).

5. DISCUSSION

It is instructive to compare the disk of 1226+0105 to that of an L^* galaxy. Following Bothun et al. (1990) we define an L^* galaxy as having a disk scale length of 3.5 kpc and a disk central surface brightness in B of 21.65 mag arcsec^{-2}. These parameters yield a disk $M_B = -19.7$, which is the value of an L^* galaxy disk derived by Efstathiou, Ellis, & Peterson (1988) for our adopted distance scale. A typical disk therefore has an

TABLE 4

H I PROPERTIES

Parameter	Malin 1	F568-6	1226+0105
Velocity (km s^{-1})	24750	13830	23660
$\Delta V_{20}(0)$ (km s^{-1})	455	674	405 ± 55
H I Mass ($M_\odot$)	1.1×10^{11}	$2\text{–}3 \times 10^{10}$	1.9×10^{10}
Dynamical mass ($M_\odot$)	2.2×10^{12}	0.9×10^{12}	1.8×10^{12}

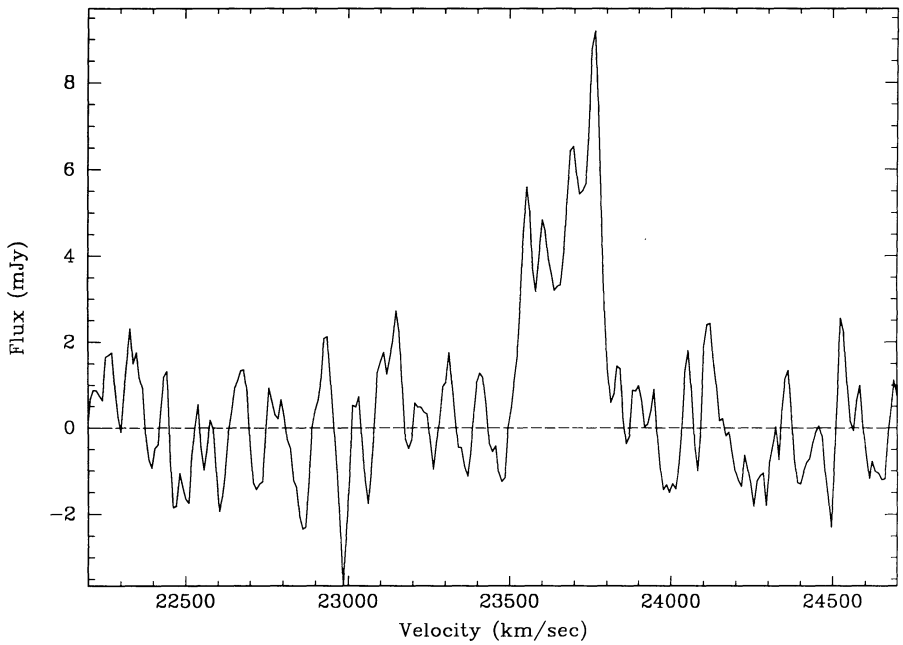

FIG. 8.—21 cm spectrum of 1226+0105, after smoothing and baseline subtraction

average B luminosity density within one scale length, of 75 $L_{\odot}$ pc^{-2}. In contrast, the disk of 1226+0105 has an average disk B luminosity density of $\sim 10\ L_{\odot}$ pc^{-2} within one scale length. If the disk $(M/L)_B$ of 1226+0105 is similar to that of an L^* galaxy, then its disk evolution should be very slow at such a low-mass density level. (Talbot & Arnett 1975; Kennicutt 1989).

Comparison of 1226+0105 to other spiral galaxies reported in the literature underscores the uniqueness of these giant LSB disks. As can be seen from Figure 9, 1226+0105 and F568-6 have central surface brightnesses as faint, and scale lengths as large, as any other spirals previously reported except for Malin 1. It is noteworthy that, except for Malin 1, the other galaxies with low central surface brightnesses have relatively short scale lengths, and those with long scale lengths have relatively high central surface brightnesses. Thus 1226+0105, F568-6, and Malin 1 seem to constitute a new class of truly giant, truly LSB disk galaxies, although Malin 1 remains the most extreme example of this class. Another characteristic of the class is a large total H I mass. Figure 10 shows that all three galaxies are

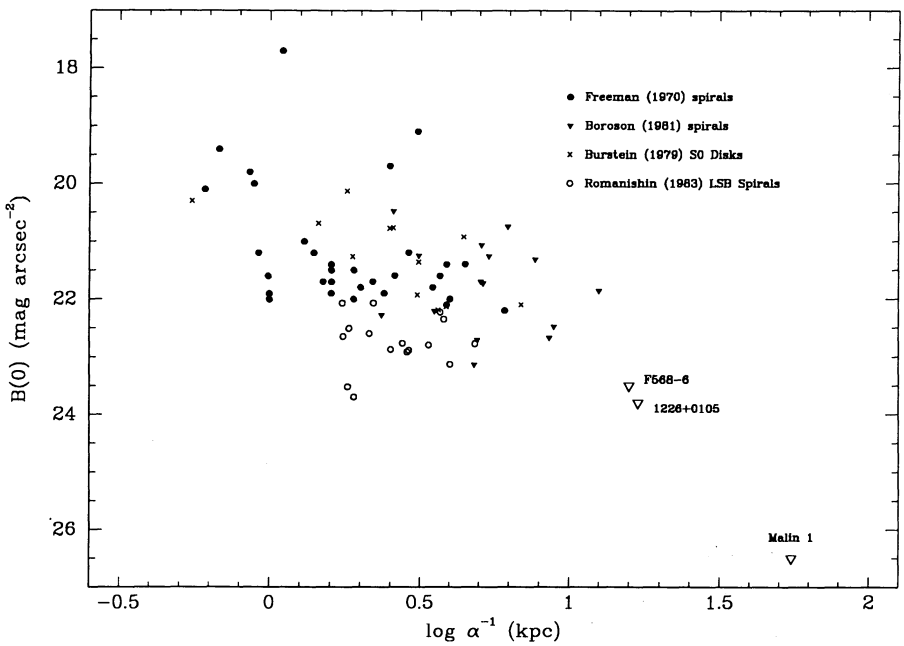

FIG. 9.—Comparison of the disk scale lengths and central surface brightnesses of Malin 1, F568-6, and 1226+0105 with previously studied spiral galaxy disks

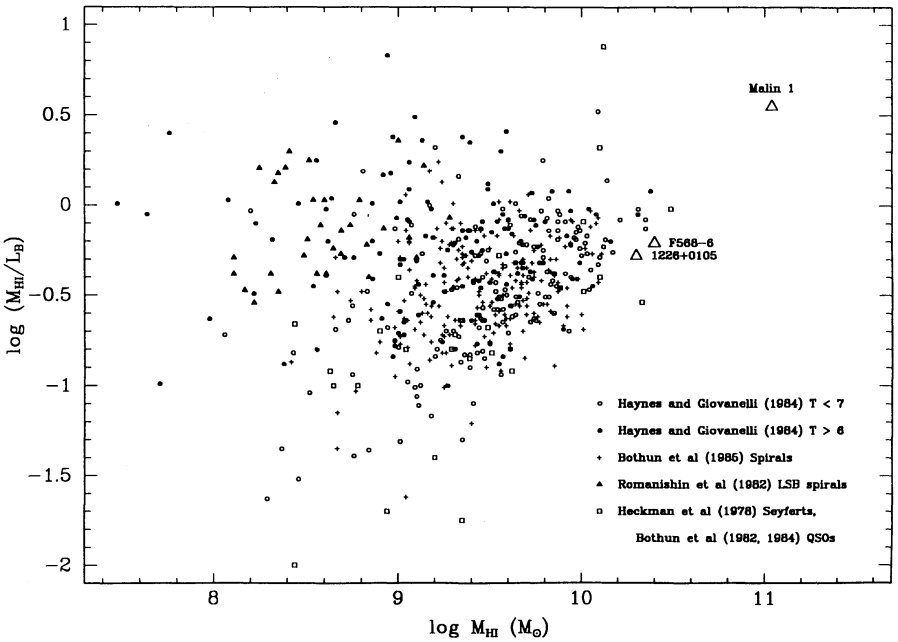

FIG. 10.—Comparison of the H I masses and blue luminosities of Malin 1, F568-6, and 1226+0105 with those of previously studied spiral galaxies. The blue luminosities plotted for Malin 1, F568-6, and 1226+0105 are for the disks only to avoid biasing the ratio by inclusion of the AGN. The luminosities for the Seyfert galaxies and QSOs also exclude the nuclear luminosity wherever possible.

at the high-mass end of the distribution of spiral galaxies in total H I mass, and that Malin 1 contains several times more H I than the next most gas-rich galaxies. Malin 1 also has a very high ratio of H I mass to blue luminosity. However, 1226+0105 and F568-6 have $M_{\rm H\,I}/L_B \sim 0.6$, which is only about 20% that of Malin 1 and is well within the range of reported spiral galaxies. Therefore, while large total H I mass is a characteristic of giant LSB disk galaxies, an unusually high $M_{\rm H\,I}/L_B$ ratio is not.

The formation of giant LSB disks was the subject of a recent theoretical paper by Hoffman, Silk, & Wyse (1992). They proposed that LSB disks originate as rare (3 σ) density peaks located within low-density regions. For the highest density peaks in the lowest density backgrounds, they found that the resulting galactic disks should resemble the disk of Malin 1. In particular, they predicted that such galaxies should have normal bulges but unevolved disks. They also predicted that these galaxies should have rotation curves that rise steeply over the inner radii and then flatten out at velocities of $\sim$300 km s^{-1}.

These predictions are consistent with the present data on LSB disks. Malin 1, F568-6, and 1226+0105 all have bright (compared to their disks) bulges that exhibit classic $r^{1/4}$ profiles. The bulges of Malin 1 and 1226+0105 are also redder ($B-V \sim 1$) than their disks. Thus their bulges can be described as normal. Also, all three galaxies show peak rotational velocities of $\lesssim$300 km s^{-1} from their H I line widths, where we take $V_r = W_0/2$. However, it is not possible to say from the present evidence whether their disks are "unevolved." The clearest gauges of disk evolution would be spectral measures of metallicity, but spectra at suitable resolution and signal-to-noise ratio of a disk with $\mu_B \gtrsim 25$ mag arcsec^{-2} are probably beyond the capability of current instruments. All three have large masses of H I available to fuel star formation, but F568-6 and 1226+0105 have disk ratios of $M_{\rm H\,I}/L_B < 1$, suggesting that they have already processed a significant fraction of their primordial gas into stars.

Hoffman et al. predicted that these attributes should be most pronounced for galaxies located in very underdense regions. Impey & Bothun (1989) noted that Malin 1 appeared to be in a low-density region, based on their estimated empty volume around Malin 1 of 9200 Mpc^3 before a nearest bright neighbor was reached, or about 13 Mpc away. Unfortunately, the volume of space at high velocities is sampled only for the most luminous galaxies, even in the well-studied direction of the Virgo cluster (where Malin 1 was found). For example, the 1990 October release of the Center for Astrophysics Redshift Survey has an average density (after subtraction of one cluster) of one galaxy 33,300 Mpc^{-3} within the declination range $-4° \leq \delta \leq +4°$ and the redshift range 20,000 km s^{-1} $\leq z \leq$ 30,000 km s^{-1}. Present redshift catalogs cannot answer the specific question of whether 1226+0105 lies in a low-density region. Recent work by Bothun et al. (1993) confirms that LSB galaxies are statistically less likely to have companions than are high surface brightness galaxies, and Zaritsky & Lorrimer (1993) find an average number of companions to LSB galaxies that is not significantly different from zero. It therefore seems likely that, as Hoffman et al. predict, the environment of these LSB disks is primarily responsible for their appearance.

6. CONCLUSION

Like the two previously described giant LSB disk galaxies, 1226+0105 is both large and luminous. The total H I mass and L_B are typical of the largest spirals, but its long scale length and low central surface brightness in optical wavelengths make it difficult to detect behind the obscuring foreground haze of the night sky. Unlike its cousins Malin 1 and F568-6, 1226+0105 has some evidence of complex color variations within its disk

suggesting a more complex star formation history in the disk. Furthermore, 1226+0105 appears to harbor an active nucleus similar to Malin 1 and F568-6, but at the same time closer in characteristics to a Seyfert I nucleus.

The authors wish to acknowledge the skillful and good-humored assistance of the staffs at the Arecibo Observatory, the Isaac Newton Group of Telescopes, the Multiple Mirror Telescope, and the Steward Observatory Kitt Peak Station. The authors thank C. B. Foltz and J. Beiging for their constructive review of an early draft of this paper, and Hans-Walter Rix for his helpful comments on the surface photometry. This work was supported by National Science Foundation grant AST 90-03158. D. Sprayberry was supported by a National Science Foundation Graduate Research Fellowship.

REFERENCES

Boroson, T. 1980, Ph.D. thesis, Univ. Arizona
Boroson, T. 1981, ApJS, 46, 177
Bothun, G. D., Heckman, T., Schommer, R. A., & Balick, B. 1984, AJ, 89, 1293
Bothun, G. D., Impey, C. D., & Malin, D. F. 1991, ApJ, 376, 404
Bothun, G. D., Impey, C. D., Malin, D. F., & Mould, J. R. 1987, AJ, 94, 23
Bothun, G. D., Mould, J., Heckman, T., Balick, B., Schommer, R. A., & Kristian, J. 1982, AJ, 87, 1621
Bothun, G. D., Schommer, R. A., Aaronson, M., Mould, J., Huchra, J., & Sullivan, W. 1985, ApJS, 57, 423
Bothun, G. D., Schombert, J. M., Impey, C. D., & Schneider, S. E. 1990, ApJ, 360, 427
Bothun, G. D., Schombert, J. M., Impey, C. D., Sprayberry, D., & McGaugh, S. 1993, AJ, submitted
Burstein, D. 1979, ApJ, 234, 435
Burstein, D., Faber, S. M., Gaskell, C. M., & Krumm, N. 1984, ApJ, 287, 586
Burstein, D., & Heiles, C. 1978, ApJ, 225, 40
Christian, C. A., Adams, M., Barnes, J. V., Butcher, H., Hayes, D. S., Mould, J. R., & Siegel, M. 1985, PASP, 97, 363
Coleman, G. D., Wu, C.-C., & Weedman, D. W. 1980, ApJS, 43, 393
Davies, J. I., Phillips, S., Cawson, M. G. M., Disney, M. J., & Kibblewhite, E. J. 1988, MNRAS, 232, 239
Efstathiou, G., Ellis, R., & Peterson, B. 1988, MNRAS, 232, 431
Freeman, K. 1970, ApJ, 160, 811
Hardie, R. H. 1962, in Stars and Stellar Systems, Vol. 2, Astronomical Techniques, ed. W. A. Hiltner (Chicago: Univ. Chicago Press), 178
Haynes, M. P., & Giovanelli, R. 1984, AJ, 89, 758
Heckman, T., Balick, B., & Sullivan, W. 1978, ApJ, 224, 745
Hoffman, Y., Silk, J., & Wyse, R. F. G. 1992, ApJ, 388, L13
Impey, C. D., & Bothun, G. D. 1989, ApJ, 341, 89
Impey, C. D., Bothun, G. D., & Malin D. F. 1988, ApJ, 300, 634
Irwin, M. J., Davies, J. I., Disney, M. J., & Phillipps, S. 1990, MNRAS, 245, 289
Jedrzejewski, R. I. 1987, MNRAS, 226, 747
Kennicutt, R. C. 1989, ApJ, 344, 685
Kibblewhite, E. J., Bridgeland, M. T., Bunclark, P. S., & Irwin, M. J. 1984, in Astronomical Microdensitometry Conf., ed. D. A. Klinglesmith (NASA CP-2317), 277
Massey, P., Strobel, K., Barnes, J. V., & Anderson, E. 1988, ApJ, 328, 315
Osterbrock, D. 1977, ApJ, 215, 733
———. 1989, Astrophysics Of Gaseous Nebulae And Active Galactic Nuclei (Mill Valley: Univ. Science Books)
Osterbrock, D., Koski, A., & Phillips, M. 1976, ApJ, 206, 898
Pence, W. 1976, ApJ, 203, 39
Romanishin, W., Krumm, N., Salpeter, E., Knapp, G., Strom, K., & Strom, S. 1982, ApJ, 263, 94
Romanishin, W., Strom, K., & Strom, S. 1983, ApJS, 53, 105
Sandage, A., & Binggeli, B. 1984, AJ, 89, 919
Schombert, J. M., & Bothun, G. D. 1988, AJ, 95, 1389
Schombert, J. M., Bothun, G. D., Schneider, S. E., & McGaugh, S. S. 1992, AJ, 103, 1107
Talbot, R., & Arnett, D. 1975, ApJ, 197, 551
van Gorkom, J., Bothun, G. D., & Impey, C. D. 1993, in preparation
Zaritsky, D., & Lorrimer, S. 1993, ApJ, in preparation